JTTEE5 9:354-359

Development of Thermal Spraying-Sintering Technology for Solid Oxide Fuel Cells

K. Okumura, Y. Aihara, S. Ito, and S. Kawasaki

(Submitted 17 December 1999; in revised form 7 April 2000)

A thermal spraying-sintering process has been developed for an electrolyte and interconnect layer, which results in improved gas tightness, a thinner layer, and higher electric conductivity as required for solid oxide fuel cells (SOFCs). The process is characterized by the heat treatment of composition-controlled plasma-sprayed layers. For the electrolyte, the addition of MnO_2 to zirconia powder is effective for reducing the sintering temperature to obtain gas tightness and for suppressing the reaction between zirconia and air electrode material. An electrolyte layer of 60 μm thickness with sufficient gas tightness and high ionic conductivity was obtained by this process. For the interconnect, chromium-rich lanthanum chromite powder, $La_{0.8}Ca_{0.2}Cr_{1.10}O_3$, is optimum for both gas tightness and high electric conductivity of the layer. In addition, a single cell with a 60 μm electrolyte was successfully fabricated using the thermal spraying-sintering process. As a result of an operating test using O_2 and humidified H_2 at 1000°C, a power density of 0.73 W/cm^2 was obtained. It was demonstrated that the thermal spraying-sintering technology is effective for the fabrication of a thin gas tight layer for SOFCs.

Keywords fuel cell, gas tightness, lanthanum chromite, plasma spray, sintering, thermal spray, zirconia

1. Introduction

Solid oxide fuel cells (SOFCs) are drawing much interest as a power generation system because of their high power generation efficiency and the low impact they impose on the environment.[1] The basic structure of a SOFC consists of an electrolyte layer in contact with an air electrode and a fuel electrode on each side, and an interconnect layer between adjacent cells. The electrolyte and interconnect must be gas tight to separate the fuel and oxidant and must be thin to reduce the internal resistance of the cell. In addition, they must be chemically stable under the operating condition of SOFCs.

The plasma spray process is more attractive because of its fast deposition rate and easy masking for deposition of patterned structures, compared with other film formation processes such as electrochemical vapor deposition, chemical vapor deposition, and sputtering. Therefore, the plasma spray process is being considered as a means of reducing manufacturing cost.

However, ceramic coatings may contain microcracks induced by shrinkage during the cooling of the deposit and pores due to the entrainment of air in the deposit.[2,3] Furthermore, coatings of perovskite oxide, in particular, doped lanthanum chromite, may change in chemical composition from the powder and exhibit chemical heterogeneity due to the material volatility in the plasma arc.[2] These problems must be avoided in order to obtain gas tightness, high electric conductivity, and matching of thermal expansion coefficients as required for SOFCs.

A sintering process has been investigated following plasma spraying, which is described hereafter as the "thermal spraying-sintering process," to obtain improved gas tightness, a thinner layer, and higher electric conductivity of the electrolyte and interconnect layers.[4,5] In this process, chemical composition of the powder and sintering temperature are important factors to control the properties of the layer. The principal objective of this study was to determine the optimum composition of the powder and sintering temperature for the thermal spraying-sintering process. In particular, the following items were investigated.

- Effect of sintering temperature and sintering agent (MnO_2) on both gas tightness and microstructure of a zirconia electrolyte layer.
- Effect of compositional change in the spraying on both gas tightness and microstructure of a lanthanum chromite interconnect layer.
- Evaluation of a single cell with the electrolyte layer prepared by the thermal spraying-sintering process.

K. Okumura, Y. Aihara, S. Ito, and **S. Kawasaki**, NGK Insulators, Ltd., Nagoya 467-8530, Japan. Contact e-mail: okumura@ngk.co.jp.

2. Experimental

2.1 Zirconia Electrolyte Layer

Electrolyte layers were sprayed using an atmospheric plasma spraying system manufactured by Plasma-Technik AG Switzerland (PT-M1100C). Current and voltage settings of the gun (F4-MB) were 570 A and 70 V, respectively. The primary gas used was argon with an addition of 23 vol.% secondary gas of hydrogen. A spray distance of 100 mm was used in this investigation.

Table 1 shows four different approaches for spraying the electrolyte. YZ-1 is the simple spraying of a commercially available 8 mol.% Y_2O_3-stabilized ZrO_2 (YSZ) powder. YZ-2 and YZ-3 are aimed at both reducing the sintering temperature and suppressing the reaction between the zirconia and the air electrode material. YZ-2 is the spraying of MnO_2 (precoating) followed by the spraying of YSZ, while YZ-3 consists of spraying MnO_2-added YSZ. For YZ-1, YZ-2, and YZ-3, the deposits were plasma sprayed onto lanthanum manganite porous substrates. Subsequently, the sprayed layers were sintered with the sub-

Table 1 Spray process for the deposition of the electrolyte

Number	Powder specification
YZ-1	YSZ(a)
YZ-2	MnO_2 (precoating 3 mg/cm^2), YSZ(a)
YZ-3	MnO_2-added YSZ(a) (5 wt.%)
YZ-4	YSZ(b)

(a) Particle size: 10 ~ 45 μm
(b) Average particle size: 0.3 μm

Table 2 Specifications of lanthanum chromite powders

Number	Selected chemical composition
LC-1	$La_{0.8}Ca_{0.2}Cr_{0.95}O_{3-\delta}$
LC-2	$La_{0.8}Ca_{0.2}Cr_{1.00}O_{3-\delta}$
LC-3	$La_{0.8}Ca_{0.2}Cr_{1.05}O_{3-\delta}$
LC-4	$La_{0.8}Ca_{0.2}Cr_{1.10}O_{3-\delta}$
LC-5	$La_{0.8}Ca_{0.2}Cr_{1.15}O_{3-\delta}$

strates, in the temperature range of 1000 to 1550 °C for 3 h in air. In addition, process YZ-4 was used for preparing a reference using a conventional pressing-sintering method at 1500°C for 3 h in air.

The N_2 gas permeability of the layer was measured at a pressure of 0.1 kg/cm^2 to evaluate gas tightness. The microstructure, chemical composition, and crystalline phase of the layers were examined by scanning electron microscopy, inductively coupled plasma spectrometry, and x-ray diffraction (XRD), respectively. The ionic conductivity of the layer was measured by the AC impedance method.

2.2 Lanthanum Chromite Interconnect Layer

Table 2 shows the chemical compositions of lanthanum chromite powders for the interconnect. La_2O_3, $CaCO_3$, and Cr_2O_3 powders were weighed in proportions, as indicated in Table 2, and finely ground on a grinding bench for about 24 h and thoroughly mixed. The mixture was sintered at 1300 °C for 5 h in air. The sintered material was subsequently broken up and finely ground in a motor mill. Then, the sieve fractions (particle size: 45 ~ 105 μm) were sprayed onto lanthanum manganite porous substrates using current and voltage settings of 570 A and 70 V, respectively. Plasma spraying system and process parameters were the same as those used for the electrolyte layers described above. The sprayed layers of LC-3, LC-4, and LC-5 were sintered with the substrates at 1500 °C for 5 h in air.

The N_2 permeability, microstructure, chemical composition, and crystalline phase of the layers were examined in a manner similar to the zirconia electrolyte described above. Electric conductivity was measured by the DC four-terminal method.

2.3 Cell Evaluation

A single cell with the electrolyte layer was fabricated by the thermal spraying-sintering process. The cell design is shown in Fig. 1.[6] The 5 wt.% MnO_2-added YSZ powder was plasma sprayed onto the air electrode substrate. The layer (60 μm) was subsequently sintered at 1400°C for 3 h in air to achieve gas tightness of the electrolyte layer. Ni-YSZ was used for the fuel electrode. The cell size was 50 mm in length × 21 mm in width × 6 mm in thickness. The active electrode area was 10.8 cm^2.

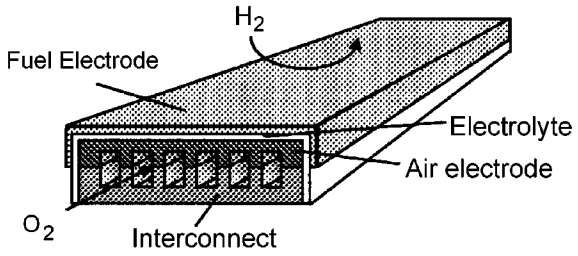

Fig. 1 Design of a long monolithic planar cell

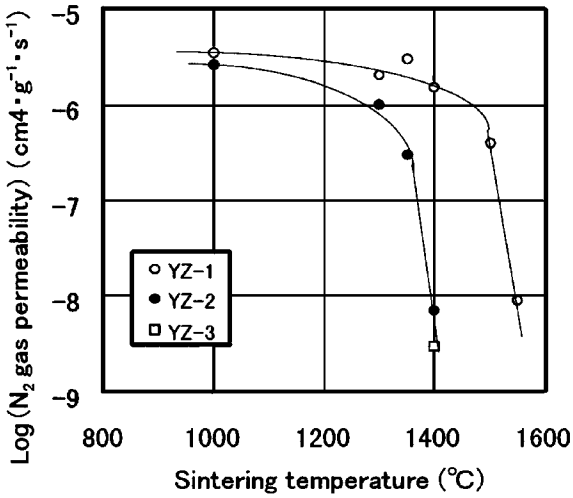

Fig. 2 Effect of sintering temperature on N_2 gas permeability of the electrolyte layer

A single cell was tested at 1000°C using O_2 and H_2-3% H_2O as the oxidant and fuel, respectively. The performance was evaluated in terms of an open-circuit voltage (OCV) and a maximum power density obtained from voltage-current characteristics.

3. Results and Discussion

3.1 Zirconia Electrolyte Layer

The effect of the sintering temperature on N_2 gas permeability is shown in Fig. 2. In the spraying of YSZ (YZ-1), the permeability of the layer decreases suddenly above 1500°C and reaches a value of less than 1×10^{-8} cm^4·g^{-1}·s^{-1} at 1550 °C. It was confirmed that gas tightness could be improved by the sintering process of the sprayed layer. On the other hand, for the process of spraying YSZ with MnO_2 precoating (YZ-2), and the process of spraying MnO_2 together with YSZ (YZ-3), the permeability values decrease at a lower temperature of 1400°C. The existence of MnO_2 in the sintering stage was effective in reducing the temperature required to obtain sufficient gas tightness.

The microstructures of the layers are shown in Fig. 3. Numerous microcracks and pores are observed in the spraying of YSZ (a), while in the spraying-sintering of YSZ (1550°C), microcracks have disappeared and spherical closed pores have formed (b). The sudden decrease of permeability at 1550°C is

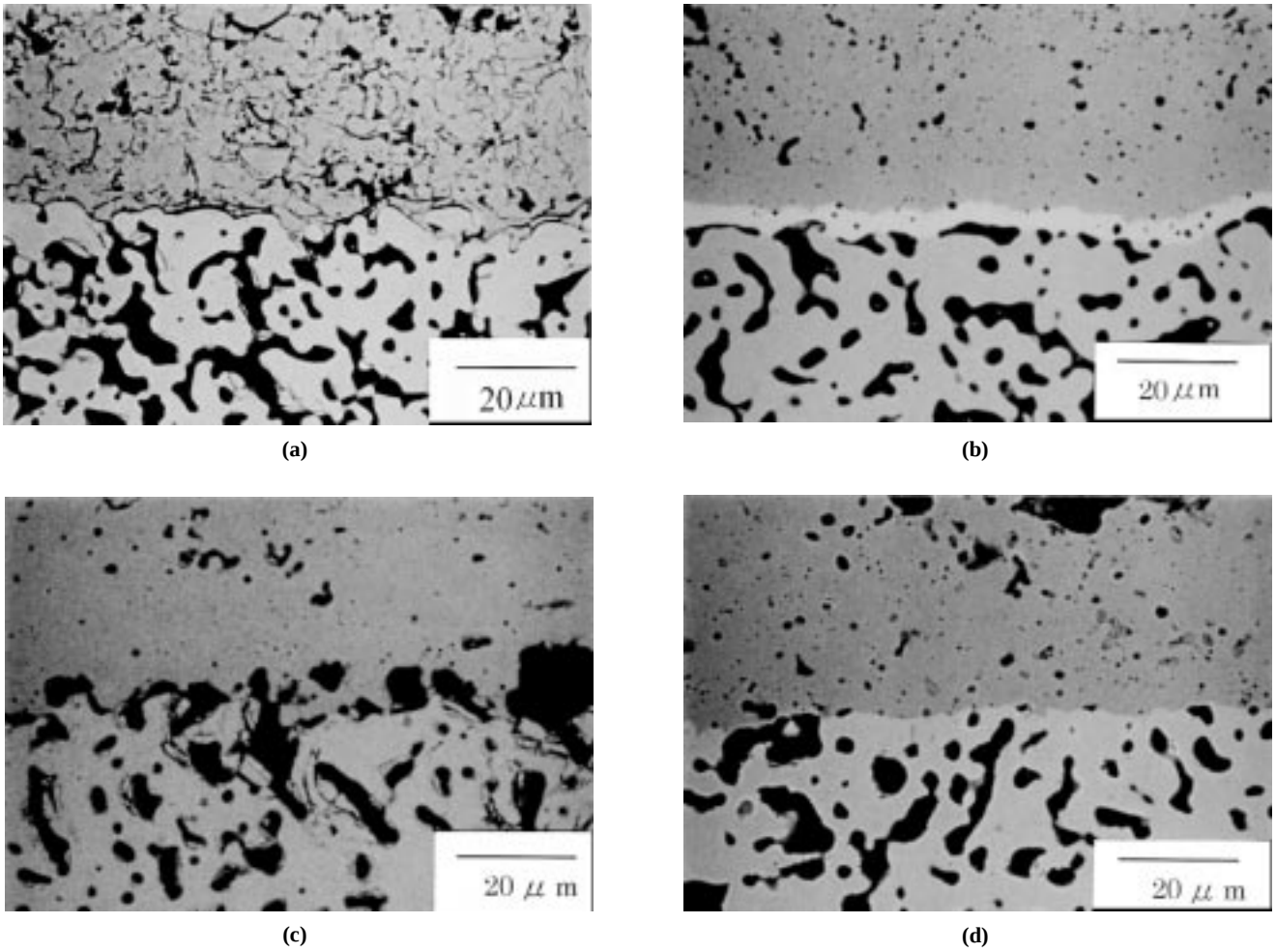

Fig. 3 Backscattered scanning electron micrographs of polished cross sections of the electrolyte layer on the air electrode. (**a**) Spraying of YSZ (YZ-1), (**b**) spraying-sintering of YSZ (YZ-1, 1550 °C), (**c**) spraying-sintering of YSZ with MnO_2 precoating (YZ-2, 1400 °C), and (**d**) spraying-sintering of MnO_2-added YSZ (YZ-3, 1400 °C)

considered to be due to the change in pore shape from open microcracks to spherical closed pores upon sintering. However, a reaction product (white part), consisting of a $La_2Zr_2O_7$ insulating layer, was observed at the electrolyte/air electrode interface. This product is undesirable because it increases the internal resistance of the cell. In the spraying-sintering of YSZ with MnO_2 precoating, spherical closed pores have formed at a lower temperature of 1400°C (c) and the reaction product was not observed. However, some MnO_2 (dark part) remained at the interface. In the spraying-sintering of MnO_2 together with YSZ (d), spherical closed pores have formed, while neither the reaction product nor MnO_2 was observed. The reason why $La_2Zr_2O_7$ was produced at the interface is believed to be related to the fact that Mn in $LaMnO_3$ diffuses into YSZ to form a solid solution of MnO and YSZ, while the remaining La reacts with ZrO_2 to produce $La_2Zr_2O_7$. The existence of a proper content of Mn in the layer suppresses the Mn diffusion, which eliminates the reaction.

In this process, the change in pore shape results in the observed gas tightness. The porosity of the layer probably does not change, and, consequently, no shrinkage of the layer occurs during sintering. Thus, separation of the layer was not observed,

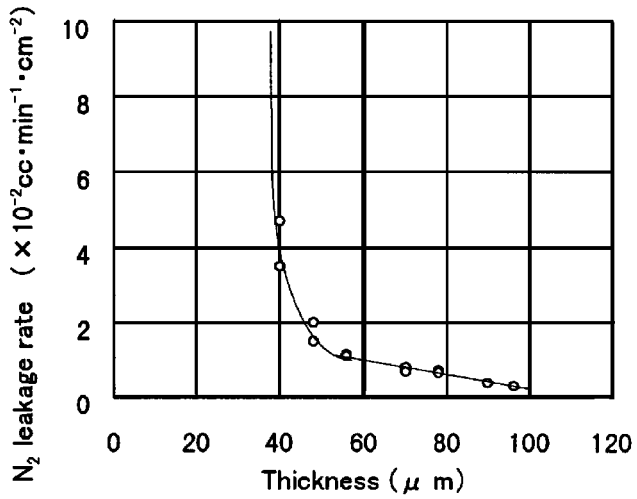

Fig. 4 N_2 leak rate vs thickness of the spray-sintered electrolyte

which is an advantage of this process over the conventional cosintering with a combination of a green body and a slurry coating.

Figure 4 shows the relationship between the N_2 leakage rate and the thickness of the layer in the spraying-sintering of MnO_2-

Table 3 Chemical composition, crystalline phase, and properties of zirconia layers

Process	Powder	Chemical composition (wt.%) ZrO_2 Y_2O_3 MnO_2	Crystalline phase	Thermal expansion coefficient (10^{-6} K^{-1})(a)	Ionic conductivity (S/cm)(b)
Conventional pressing-sintering	YZ-4	83.2 13.9 0	C	10.4	0.14
Spraying-sintering 1400 °C × 3 h	YZ-3	81.1 14.5 3.8	C	9.9	0.12

C: Cubic single phase
(a) 40 to 1000 °C
(b) 1000 °C

Table 4 N_2 gas permeability of the interconnect layers (100 μm in thickness)

Process	Powder	N_2 gas permeability ($cm^4 \cdot g^{-1} \cdot s^{-1}$)
Spraying	LC-3	1.6×10^{-6}
	LC-4	1.6×10^{-6}
	LC-5	2.0×10^{-6}
Spraying-sintering (1500 °C × 5 h)	LC-3	1.0×10^{-8}
	LC-4	5.0×10^{-8}
	LC-5	5.0×10^{-7}

added YSZ. The leakage rate was very low for a thickness greater than 50 μm, but for a thickness less than 50 μm, the leakage rate suddenly increased, probably due to incomplete overlapping of the deposits. It was confirmed that a 50 μm layer with sufficient gas tightness could be obtained by this process.

The properties of the layers are given in Table 3, including the chemical composition of the layer. The properties of the layer formed by the spraying-sintering process were comparable to those of the layer formed by a conventional pressing-sintering process.

3.2 Lanthanum Chromite Interconnect Layer

The N_2 gas permeability of the lanthanum chromite interconnect layer is given in Table 4. In the thermal spraying-sintering, very low permeabilities of 1 to 5×10^{-8} $cm^4 \cdot g^{-1} \cdot s^{-1}$ were obtained for LC-3 and LC-4. Gas tightness of the sprayed lanthanum chromite layer was improved by the sintering process similarly to the above zirconia case. However, in the spraying-sintering of LC-5, the gas tightness was not improved.

The microstructures of the layers are shown in Fig. 5. In the spraying of LC-4 (a), numerous microcracks and pores are observed, while in the spraying-sintering of LC-3 (b) and LC-4 (c), only spherical pores are observed. However, in the spraying-sintering of LC-5 (d), much smaller pores were observed, indicating that the layer has lower sinterability. Therefore, when using a proper composition of the powder, change in pore shape and pore growth occurred during sintering, which resulted in the lower N_2 gas permeability.

The chemical compositions of the layers are given in Table 5. During the spraying, the chromium content decreased compared to the original powder in each case, but no further change occurred during the sintering step. The decrease of chromium content in the spraying process is considered to be due to the high volatility of chromium oxide in the plasma jet.

The crystalline phases of the layers are also given in Table 5. The XRD peaks from sprayed-sintered layers are narrower than those from the sprayed layers. This implies that crystallinity was improved after the sintering process. In the spraying-sintering process, a perovskite single phase was obtained only for LC-4, while CaO and Cr_2O_3 were detected for LC-3 and LC-5, respectively. As can be seen from the results of the conventional pressing-sintering process, the equilibrium nonstoichiometric range is narrow. It appears that $\chi = 0.95$ and 1.05 (χ in $(La,Ca)Cr_{1-x}O_3$) may be beyond the nonstoichiometric range at 1500°C. Judging from the results of microstructural observations, precipitated Cr_2O_3 may suppress the sintering of lanthanum chromite.

The electric conductivities of the layers are also given in Table 5. It was confirmed that the electric conductivity of each layer was increased by the sintering process. This increase can be explained by both the microcrack disappearance and the crystallinity improvement upon sintering.

The use of chromium-rich lanthanum chromite powder is preferable for compensating the chromium deficiency in the spraying process and also for avoiding CaO precipitation in the sintering process, while excess chromium in the sprayed layer will inhibit the improvement of gas tightness. Therefore, the optimum composition of the lanthanum chromite powder must be selected in this thermal spraying-sintering process. In this study, $\chi = 1.10$ (LC-4) was selected as the optimum composition of the powder. However, this value may depend on such factors as the particle size and plasma-spray conditions. The understanding of these effects is an important subject for future studies.

3.3 Cell Evaluation

Figure 6 shows current density/voltage and current density/power density characteristics of the cell when the cell was operated at 1000°C. An OCV of 1060 mV was obtained, which is very close to the theoretical value calculated from the supplied-gas composition. This result implies sufficient gas tightness in the 60 μm electrolyte layer fabricated by the spraying-sintering process. The maximum power density of 0.73 W/cm^2 was obtained at 0.49 V and 1.50 A/cm^2. The result implies that very low internal resistance was realized through the use of the very thin electrolyte layer. It was demonstrated that the thermal spraying-sintering technology is effective for fabrication of thin gas-tight layer for SOFCs.

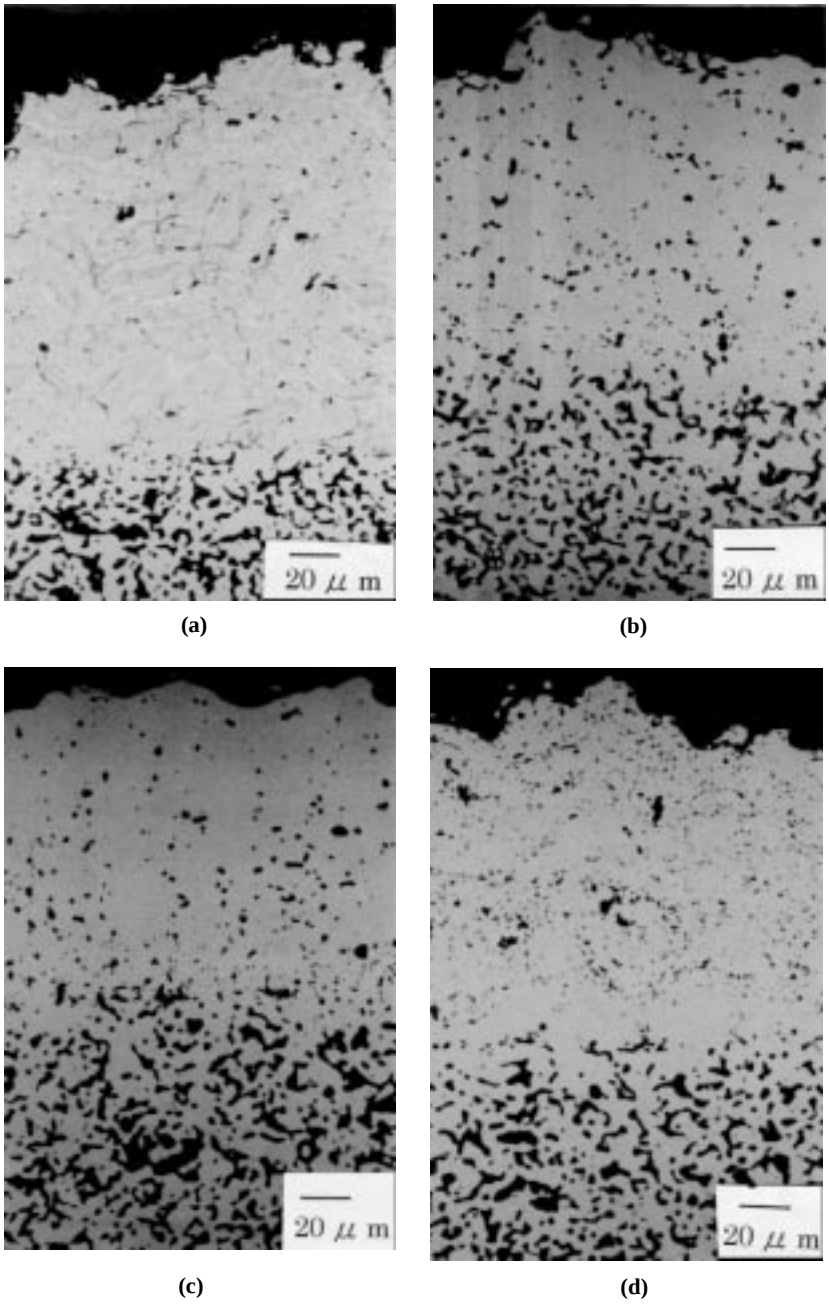

(a) **(b)** **(c)** **(d)**

Fig. 5 Backscattered scanning electron micrographs of polished cross sections of the lanthanum chromite interconnect layer on the air electrode. (**a**) Spraying of LC-4, (**b**) spraying-sintering of LC-3 (1500 °C), (**c**) spraying-sintering of LC-4 (1500 °C), and (**d**) spraying-sintering of LC-5 (1500 °C)

4. Conclusions

A thermal spraying-sintering process has been developed for achieving an improved gas tightness, thinner layer, and higher electric conductivity of electrolyte and interconnect of SOFCs.

- The use of MnO_2-added YSZ powder is effective for both reducing the sintering temperature to obtain gas tightness and suppressing reaction between zirconia and the air electrode material. A zirconia electrolyte layer of 60 μm thickness, fabricated by this process, exhibits improved gas tightness and high ionic conductivity, which satisfy the requirements of SOFCs.
- Chromium-rich lanthanum chromite powder is required in the thermal spraying-sintering process, in order to obtain an interconnect layer with both gas tightness and chemical homogeneity. In this experiment, $La_{0.8}Ca_{0.2}Cr_{1.10}O_3$ was selected as the optimum composition. A lanthanum chromite interconnect layer of 100 μm thickness, fabricated by this process, exhibited improved gas tightness, chemical homogeneity, and higher electric conductivity, which are desirable for SOFCs.

Table 5 Chemical, crystalline phase, and properties of lanthanum chromite layers

Process	Powder	Chemical composition	Crystalline phase	Thermal expansion coefficient 10^{-6} °C^{-1}(a)	Electric conductivity S/cm (b)
Conventional pressing-sintering	LC-1	$La_{0.80}Ca_{0.20}Cr_{0.95}O_{3-\delta}$	P + CaO	9.9	31.2
	LC-2	$La_{0.80}Ca_{0.20}Cr_{1.00}O_{3-\delta}$	P	9.9	—
	LC-3	$La_{0.80}Ca_{0.20}Cr_{1.07}O_{3-\delta}$	P + Cr_2O_3	9.7	—
Spraying	LC-3	$La_{0.8}Ca_{0.2}Cr_{0.95}O_{3-\delta}$	P (broad)	—	30.6
	LC-4	$La_{0.8}Ca_{0.2}Cr_{1.00}O_{3-\delta}$	P (broad)	—	19.3
	LC-5	$La_{0.8}Ca_{0.2}Cr_{1.05}O_{3-\delta}$	P (broad)	—	28.8
Spraying-sintering (1500 °C × 5 h)	LC-3	$La_{0.8}Ca_{0.2}Cr_{0.95}O_{3-\delta}$	P + CaO	9.7	42.2
	LC-4	$La_{0.8}Ca_{0.2}Cr_{1.00}O_{3-\delta}$	P	10.0	28.2
	LC-5	$La_{0.8}Ca_{0.2}Cr_{1.03}O_{3-\delta}$	P + Cr_2O_3	9.8	34.2

P: perovskite
(a) 40 to 1000 °C
(b) 1000 °C
—not measured

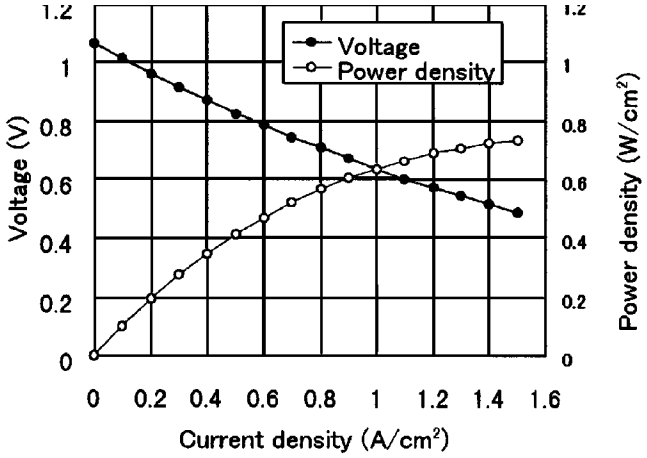

Fig. 6 Electrical performance of a single cell with an electrolyte layer prepared by the spraying-sintering process

- A single cell with the 60 μm electrolyte was successfully fabricated using the thermal spraying-sintering process. As a result of an electrical performance test, a high power density of 0.73 W/cm^2 at 1000°C was achieved. It was demonstrated that the thermal spraying-sintering technology is effective for the fabrication of the layers having the high performance required for SOFCs.

References

1. S.C. Singhal: *Proc. 5th Int. Symp. on Solid Oxide Fuel Cells,* U. Stimming, S.C. Singhal, H. Tagawa, and W. Lehnert, eds., The Electrochemical Society, Inc., Pennington, NJ, 1997, p 37-50.
2. E.R. Ray, C.J. Spengler, and H. Herman: *Solid Oxide Fuel Cell Processing Using Plasma Arc Spray Deposition Techniques,* DOE/mc/25167-2986, DOE METEC, Morgantown, WV, July 1991.
3. Z. Li, M. Behruzi, L. Fuerst, and D. Stover: *Proc. 3rd Int. Symp. on Solid Oxide Fuel Cells,* S. C. Singhal and H. Iwahara, eds., The Electrochemical Society, Inc., Pennington, NJ, 1993, p 171-79.
4. S. Kawasaki, Y. Aihara, K. Yoshioka, T. Takahashi, and T. Soma: *Proc. 3rd Int. Symp. on Solid Oxide Fuel Cells,* S.C. Singhal and H. Iwahara, eds., The Electrochemical Society, Inc., Pennington, NJ, 1993, p 385-94.
5. Y. Aihara, S. Ito, and S. Kawasaki: *Proc. 4th Int. Symp. on Solid Oxide Fuel Cells,* Y. Dokiya, O. Yamamoto, H. Tagawa, and S.C. Singhal, eds., The Electrochemical Society, Inc., Pennington, NJ, 1995, p 180-86.
6. S. Kawasaki, K. Okumura, Y. Esaki, M. Hattori, Y. Sakaki, J. Fujita, and S. Takeuchi: *Proc. 5th Int. Symp. on Solid Oxide Fuel Cells,* U. Stimming, S.C. Singhal, H. Tagawa, and W. Lehnert, eds., The Electrochemical Society, Inc., Pennington, NJ, 1997, p 171-79.